LBNL-…..

Published as

J. Sanders, A. Rauch, R. Mendelsberg, and A. Anders, Rev. Sci. Instrum. **82,** 093505 (2011).

http://link.aip.org/link/doi/10.1063/1.3640408

A synchronized emissive probe for time-resolved plasma potential measurements of pulsed discharges

Jason M. Sanders

Department of Electrical Engineering, University of Southern California, Los Angeles, California 90089, USA

Albert Rauch, Rueben J. Mendelsberg, and André Anders

Lawrence Berkeley National Laboratory, University of California, Berkeley, California 94720, USA

Manuscript of 2011-06-30

ACKNOWLEDGMENT

Pavel Ni and Albert Rauch are gratefully acknowledged for being key on imaging the ionization zones shown in Fig. 1. I thank Rueben Mendelsberg for his comments. This work was supported by the Assistant Secretary for Energy Efficiency and Renewable Energy, Office of Building Technology of the U.S. Department of Energy (DOE) under Contract No. DE-AC02-05CH11231.

A synchronized emissive probe for time-resolved plasma potential measurements of pulsed discharges

Jason M. Sanders
Department of Electrical Engineering, University of Southern California, Los Angeles, California 90089, USA

Albert Rauch, Rueben J. Mendelsberg, and André Anders
Lawrence Berkeley National Laboratory, University of California, Berkeley, California 94720, USA

Abstract

A pulsed emissive probe technique is presented for measuring the plasma potential of pulsed plasma discharges. The technique provides time-resolved data and features minimal disturbance of the plasma achieved by alternating probe heating with the generation of plasma. Time resolution of about 20 ns is demonstrated for high power impulse magnetron sputtering (HIPIMS) plasma of niobium in argon. Spatial resolution of about 1 mm is achieved by using a miniature tungsten filament mounted on a precision translational stage. Repeated measurements for the same discharge conditions show that the standard deviation of the measurements is about 1-2 V, corresponding to 4-8% of the maximum plasma potential relative to ground. The principle is demonstrated for measurements at a distance of 30 mm from the target, for different radial positions, at an argon pressure of 0.3 Pa, a cathode voltage of -420 V, and a discharge current of about 60 A in the steady-state phase of the HIPIMS pulse.

I. INTRODUCTION

Emissive probes have been used in a variety of plasma environments to determine important plasma properties, including the plasma potential, ion density, electron density, and electron temperature.[1-3] First described by Langmuir in 1923, electron emitting probes consist of a thin metal wire filament, typically made from tungsten, that is heated to high temperature with a current in order to achieve thermionic emission.[4] When immersed in plasma, a sheath forms around the surface of the filament. The sheath thickness is governed a number of factors, including the difference between plasma potential and probe potential, and the temperature of the probe's filament which determines thermionic electron emission. Measuring the balance of electron current emitted from the probe and the particle currents to the probe provides an accurate method for determining the local potential of the plasma.

Emissive probes are often preferable to collecting probes for determining the plasma potential because emissive probes are capable of providing the measurement directly. To show the advantages, we first consider the theory of cold, non-emitting probes. The plasma potential Φ can be calculated via

$$\Phi = V_f + \frac{k_B T_e}{q} \ln\left(\frac{I_{es}}{I_{is}}\right) \tag{1}$$

where V_f, is the floating potential, T_e is the electron temperature, I_{es} is the electron saturation current, I_{is} is the ion saturation current, k_B is the Boltzmann constant, and q is the average charge of the ions. This indirect measurement technique requires knowledge of the electron temperature, which can fluctuate during the measurement, and mean ion charge state, which is often but not always close to unity. Furthermore, equation (1) is valid for electron velocity distributions that are Maxwellian, so

the calculated plasma potential will be erroneous for the highly magnetized, pulsed plasmas used in some processing techniques.

Emissive probes remove much of this uncertainty because the current measured as a function of probe bias for the emitting probe diverges from that measured for a collecting probe only when the bias voltage is less than the plasma potential. Therefore, the plasma potential can be determined by comparing an emissive probe's *I-V* curve to a collecting probe's *I-V* curve.[5] Furthermore, as the emission of the probe increases, the probe's floating potential shifts toward the plasma potential enabling time-resolved measurements of the probe potential by measuring the probe's floating voltage.[6] This shift in the floating potential can be understood by considering a modified version of Equation (1) that accounts for the current emitted from the probe, [7]

$$\Phi = V_f + \frac{k_B T_e}{q} \ln\left(\frac{I_{es}}{I_{is}+I_{em}}\right) , \qquad (2)$$

where I_{em} denotes the electron current emitted from the probe. The emission currents needs to be added to the ion saturation current because a current of (negative) electrons *emitted from* the probe is electrically equivalent to a current of (positive) ions *collected by* the probe. Equation (2) shows that the floating potential V_f of the probe approaches the plasma potential as the emitted current from the probe increases. V_f attains the plasma potential Φ for $I_{em}=I_{es}-I_{is}$. Further increase of I_{em} will not lead to a further growth of the potential of the probe, because it is saturating. A more detailed theoretical treatment of the how the floating potential behaves in the presence of electron emission can be found in previously published papers.[8]

In addition to these two methods of measuring the plasma potential, typically referred to as the *divergence point method* and the *saturated probe method*, respectively, there is the *inflection point method* where the plasma potential is readily identified by the inflection point of the characteristic via its first derivative.[5, 9, 10] This method, however, is less suitable for transient or noisy plasmas. For these plasmas, the saturated probe method is the most straight-forward way to evaluate the plasma potential. The accuracy of the measurement is typically about 1 V for well-controlled operating conditions.[10] The saturated probe method has been used successfully to make measurements in non-Maxwellian, magnetized plasmas[2, 7, 11] even as this method is susceptible to perturbations by magnetic fields, which must be taken into account. In the following section we will apply the saturated probe method and show the feasibility of pulsed heating to minimize plasma disturbance and enhance accuracy of measurements.

II. PULSED PROBE PRINCIPLE AND DESIGN

The basic principle of an emissive probe requires altering the characteristics of a single probe through thermionic emission of electrons by ohmic heating of the probe using a heating current (Fig. 1). When the probe potential is more positive than V_P, the probe current is unchanged by the emission of the thermal electrons because the emitted electrons cannot escape the probe's sheath and are repelled by the plasma and return to the probe. The temperature of the emitted electrons is equal to the wire temperature, corresponding to about 0.2 eV, which is much less than the energy of the plasma electrons. When the applied probe bias becomes negative relative to V_P, the emitted thermal electrons are accelerated away from the probe, and thus the measured probe current becomes increasingly greater until it saturates, indicating that all of the emitted electrons and arriving ions are measured, while all of the plasma electrons are repelled.

In this work, a synchronized, pulsed emissive probe measurement station has been designed to measure the potential of pulsed plasmas. In the design used here, the glowing probe tip was made from a tungsten coil taken from a Mini Mag Lite 2-cell AA flashlight xenon replacement bulb. A diamond saw was used to carefully cut the glass casing, which provided us with the 1 mm long solenoid made from a 30 μm tungsten wire conveniently attached to the socket with its two contact

pins (Fig. 2). The miniature solenoid consists of six turns, each turn having a diameter of approximately 240 μm. The bulb was push fit into a 2.5 mm diameter, 150 mm long ceramic stem and aligned in radial direction in the plasma volume (Fig. 3). Electrical connection to the probe was made via a twisted pair fed through the ceramic tube. Of course, this specific design is not critical for the operation of a pulsed, synchronized emissive probe. For other measurements, to be reported elsewhere, a simple loop of fine tungsten wire was used.

Typically, the probe's heating current is provided by an ac current source that is electrically isolated from ground via a transformer.[6, 11-13] By heating the filament with a pulse *before* the plasma pulse is generated, and switching heating off when the plasma is on, as illustrated in Figure 4, the electric field established by the forward voltage drop across the tungsten filament will not exist when the plasma is present. Pulsing the heating current allows us to use a tungsten coil filament from a miniature light bulb since without pulsing, the heating current flowing through the coil would produce a non-negligible magnetic field. This issue is avoided by the timing of heating. Calculations showed that the magnetic field of the light bulb solenoid generated by the heating current is about 16-23% of the local magnetic field of the magnetron's permanent magnets, at the locations of measurement. The ability to use filaments from a readily commercially available bulb reduces the cost of the probe and allows for simple replacement should the filament be damaged.

This pulsed emissive probe system readily integrates with common pulsed plasma processing techniques because typical plasma duty cycles are less than 20%, which leaves enough time to heat the probe's filament into strong thermionic emission during the plasma's off-time.[14] We show that the droop in thermionic emission during the discharge can be kept small, which means the emission is nearly constant, as if the probe is heated continuously. The filament can be sufficiently heated to achieve strong enough emission such that measurements can be made using the *saturated probe method* mentioned above. As an example of a practical implementation of the principle, measurements of the plasma potential will be presented for a 7.6 cm diameter Nb target that is pulsed in the high power impulse magnetron sputtering (HIPIMS) mode in argon at 0.33 Pa and 0.28 Pa.

III. PULSED PROBE CIRCUITRY

A schematic of the pulsing circuitry for the emissive probe is shown in Figure 1. It consists of a TTL pulse generator that times the heating, a power MOSFET, a ground-free dc heater power supply, a pulse transformer, diodes, a probe bias supply, and a current-sensing resistor. The MOSFET switches the heater power supply across the pulse transformer, which is necessary to electrically isolate the probe so that it can assume the potential determined by the probe bias voltage (or float in the absence of bias). Diodes are employed to rectify the output pulse and prevent $-L \cdot di/dt$ transients. When the probe is biased, a current-sensing resistor connects the common of the transformer's secondary winding to a bias voltage supply.

Given the low-voltage, low-frequency operation of this circuit, component choices are not critical. A MOSFET with a 50 V, 1 A rating is more than sufficient, but care should be taken to choose a device with small on-resistance and a package with good thermal conductivity. Since the impedance of the filament (approximately 5 Ω at 3000 K) is comparable to the MOSFET's on-resistance (between 0.75 Ω and 3 Ω depending on junction temperature and gate drive), a significant amount of power is dissipated in the MOSFET, so it must be well cooled for continuous operation. The pulse transformer needs to have sufficient mutual inductance and a high enough saturation flux density to prevent droop and/or core saturation. The average power transferred through the transformer is typically less than 5 W, so cooling is not difficult given that the transformer will not be lossy at these relatively long timescales of the pulsing scheme. There are no special requirements to the diodes; standard 50 V, 1 A Si rectifiers are sufficient. The power MOSFET was

an IRF840 500 V, 8 A; the diodes were DO-204AL 1 kV, 1 A; the ground-free heater power supply was a TENMA 72-7295 0-40 VDC, 0-3 A adjustable supply; and the probe bias supply was a KEPCO BOP72 controlled by the SignalExpress Software (we note that the circuit was built with parts and devices available in the lab, so the ratings exceed requirements in some cases). The MOSFET's gate was driven by a TENMA TGP110 TTL-pulse generator with an adjustable pulse width and repetition rate. The gate of the MOSFET was loaded with a 100 nF capacitor to slow its turn-on, which mitigates transients from switching the floating power supply to ground.

The radial position of the probe was controlled by LabView SignalExpress software driving a linear motion feedthrough with a stepper motor. The software controlled not only the positioning but synchronized the position with the measuring procedure described in the next section. The +/-10 V analog output of the NI PXIe-6341-card was amplified a factor of 10 by the KEPCO BOP72 amplifier which provided the actual probe bias voltage. By automating the measurement including the mechanical advancement of the probe, the probe's exposure to the HIPIMS plasma was minimized and detrimental effects (i.e. coatings) on filament's lifetime were reduced.

III. PROBE OPERATION

Figure 4 illustrates typical waveforms for the probe's heating pulse and emitted current. This measurement was made at a base pressure of 1×10^{-4} Pa with the probe biased at -50 V. In this example, the probe is heated with about 3.7 V for 20 ms, or about 36 mJ, which, for a -50 V bias, results in a peak emitted electron current of about 1.6 mA. The most important thing to note in Figure 4 is that the electron current collected after the heating pulse is relatively constant over the period of time that a typical plasma discharge would occur. For a 600 μs pulse the collected electron current only changes by 4% from 1.58 mA to 1.51 mA.

Accurate plasma potential measurements from the floating probe measurement technique require strong filament emission during the measurement period. The thermionic current density emitted from a metal is strongly temperature dependent, as described by the Richardson equation[15]

$$J = A_G T^2 e^{-\frac{W}{k_B T}} \ , \tag{3}$$

where J is the emitted electron current density, T is temperature, W is the metal's work function, and A_G is the Richardson's constant.

Since the filament was originally designed for its usual operation in a xenon gas environment, an experiment was conducted to investigate the filament's thermal properties in a lower pressure environment, where convection cooling does not apply. Figure 5 shows the blackbody radiation emitted by the glowing probe in vacuum for different average powers. The measurement was made using a spectrometer for the visible spectral range (Ocean Optics USB-4000). The spectrometer was set to have an integration time of 10 ms, and the software was set to average 100 scans and to apply boxcar smoothing with a width of 30 pixels. Systems losses and detector sensitivity were calibrated out of the measurements by dividing the measured data by the system's transfer function. The transfer function was determined by heating the probe with the right amount of power so its emission nearly matched the spectrum of an Ocean Optics LS-1 tungsten halogen light source with a filament temperature at 3100 K. Emission was then compared to the Planck distribution to obtain the wavelength-dependent system transfer function.

As expected, the absence of convection cooling results in higher filament temperature than with the usual filament's power rating. For each applied power, the filament temperature could be calculated by fitting the calibrated measured intensity (colored data symbols in Fig. 5) with a fitted black body radiation curve (solid black lines in Fig. 5). The resulting temperatures are displayed as curve labels. We stress that the time resolution of the measurements was 10 ms and therefore the

peak temperature of the probe could be somewhat higher than the temperature fitted to the spectral intensity curves. The validity of the temperature measurement approach was further checked by heating the filament up to the tungsten melting temperature (at 3695 K, when it stopped working, of course). Consistent with the temperatures determined by black body intensity distribution, the filament reached the tungsten melting temperate as the applied power was only 0.5 Watts, at a filament voltage drop of 1.75 V, corresponding to 58% of the bulb's rated dc operating voltage.

The pulsed probe operation is ultimately limited by the repetition rate of the discharges. As the duty cycle increases, the time available to heat the probe decreases and the amplitude of the heating pulse must turned up so that the filament reaches its emission temperature sufficiently fast (Fig. 6). An upper bound on the repetition rate has not yet been determined; the probe was run with a heating time as short as 500 µs, which would accommodate repetition rates as high as 2 kHz, which is higher than the repetition rates used in many pulsed plasma processing techniques. Further investigations are required to determine how the probe's lifetime is reduced by the repetitive thermal stress upon the many fast heating and cooling cycles. Effects like shorting by metal coating or oxidation in an oxidizing environment, if applicable, may also limit the probe's lifetime.

IV. DEMONSTRATION OF THE TECHNIQUE BY HIPIMS EXPERIMENTS

Experiments to test the probe's operation were conducted in a small diagnostic chamber with a planar magnetron that was pulsed with a SPIK2000A high voltage and high power pulse generator from MELEC GmbH (max voltage 1 kV, max. peak current 500 A). The electrical connections and gas feedthroughs to the chamber are shown in Fig. 3. The cylindrical stainless steel chamber with several Conflat® ports had an inner diameter of 35 cm and a depth of 25.4 cm. It was pumped down to a base pressure of 1×10^{-4} Pa with a Pfeiffer TMH 521 turbo pump backed with an MD 4 diaphragm pump from Vacuumbrand GmbH. During the experiments, an MKS mass flow controller supplied argon, raising the pressure to 0.28 Pa or 0.33 Pa.

A 6.25 mm thick, 7.6 cm diameter Nb target was used with an unbalanced planar magnetron (US Inc.®) and HIPIMS pulses were supplied by a high current SPIK2000A pulse generator (Melec® GmbH), capable of delivering up to 500 A peak current should the plasma impedance require it. A delay generator was used to synchronize the probe heating pulses with the discharge pulses (Fig. 3). For the data presented here, the HIPIMS discharges was operated at a repetition rate of 10 pulses per second and each pulse starting 200 µs after the end of a 20 ms heating pulse.

The magnetron was pulsed with negative voltages (relative to the grounded anode) between 400 – 600 V to create a mixed argon and niobium plasma. HIPIMS[16, 17] is a physical vapor deposition (PVD) technique that combines pulsed power systems with magnetron sputtering to produce plasmas of the target material. The peak power exceeds the average power by typically two orders of magnitude.[18]

Care must be taken when measuring the potential of magnetically confined plasmas because the motion of magnetized electrons can lead to inaccurate determinations of the potential. The helical motion of magnetized electrons is described in part by the particle's Larmor radius, given by

$$r_L = \frac{m_e v_\perp}{eB} \tag{4}$$

where m_e is the electron mass, $v_\perp$ is the component of the electron's velocity perpendicular to the magnetic field, e is the charge of the electron, and B is the magnetic field. If the Larmor radius is smaller than the probe's radius, emission from the probe reduces because a fraction of the electrons will return to the probe.[10] Measurements of the potential have been made with the probe positioned between 15 and 30 mm away from the target, which corresponds to magnetic

field strengths between 42 and 8 mT, above the racetrack, as measured with a Hall probe (F.W. Bell, Inc.). Assuming an electron temperature of 2 eV, which is approximately the temperature of the lower energy electrons in the non-Maxwellian plasma[11], this corresponds to minimum Larmor radii between 120 μm and 600 μm, which are respectively 8 and 40 times larger than the probe's radius. For positions closer than 20 mm to the target, the cathode voltage required to ignite the plasma increased, indicating that electrons emitted from the probe were perturbing the discharge. Inside of 15 mm, electron emission prevented plasma ignition completely, presumably because the physical presence of the probe interferes with the closed drift (Hall) current. Therefore, the measurements presented here to illustrate the principle were taken at a distance of 30 mm from the target.

V. RESULTS OF TEST EXPERIMENTS

As it is typical for HIPIMS discharges with constant voltage drive during the pulse, the power varies significantly depending on the operating pressure, cathode pulse amplitude, pulse width, and duty cycle. Figure 7 illustrates two different discharge modes: in the low power mode we essentially see a transient to what could be dc operation if the discharge was not terminated. In the high power mode, the current runs away, more than an order of magnitude, upon a relatively small increase in discharge voltage. The strong sensitivity of the discharge current on the applied voltage (and other parameters like magnetic field) is an expected discharge runaway feature which has been discussed in the literature.[17-19]

To measure the plasma potential, the probe bias voltage is swept over a wide range and the probe current is plotted versus the bias voltage. The saturated probe technique takes the plasma potential as the probe potential where the probe current intercepts the bias voltage axis (the emitted and received currents are equal). Figure 8 shows a typical current-voltage characteristic of a cold probe and a heated, emissive probe.

For this measurement, -400 V pulses were applied to the Nb target 200 μs synchronized after 3.7 V pulses were applied to the filament for 20 ms. The repetition rate was set to 10 pulses per second. The probe current in the *I-V* curve is the time-average of current measured across the current sensing resistor for a 200 μs time period in the steady-state part of the discharge waveform, as depicted in Fig. 7. As the bias is swept from -80 to 80 V, the current measured via the current sense resistor shown in Fig. 8 exhibit the expected response for the cold and hot (emissive) probe conditions.

The *I-V* characteristic of the cold probe shows a small ion saturation current (left side of the characteristic) and a much greater electron current (right side), a well-known consequence of the significantly different mobility of ions and electrons due to their mass difference. Under our conditions, the floating potential of the cold probe is about -16 V. As explained in conjunction with equation (2), the floating potential shifts to more positive values, approaching the plasma potential, when the probe is heated and the electron emission is sufficiently high.

When a voltage pulse of -420 V is applied to the target, the discharge took about 200 μs from the start of the pulse for the plasma to ignite, see Fig. 7. However, the delay time decreased with increasing pulse voltage, as known from the literature.[20] One sees the initial discharge current peak followed by rarefaction and steady state phase with a discharge current of about 60 A.

By monitoring the probe current during different phases of the discharge as a function of the applied probe bias voltage, the plasma potential at different times and discharge intensities can be quantified. Here we choose two distinctive points, namely the plasma potential at the discharge peak and at the end of the discharge pulse where we observe near-steady-state plasma. As discussed above, the plasma potential was defined as the voltage at zero probe current. Graphically it is the point where

the probe current crosses the dashed horizontal line as depicted in Fig. 9.

The initial time-resolved probe measurements reported here were made by sweeping the bias voltage between −35 V and + 5 V in 1 V steps, with the probe current readings per bias voltage step averaged over 10 pulses (Fig. 10).

Figure 11 shows the radial plasma potential distribution. Towards the center of the magnetron V_{Pl} is rapidly increased to values of -10 V, and we observe about -30 V in region of the target's racetracks, where the electrons are trapped by the magnetic field lines. The investigations thus showed that the radial plasma potential distribution is strongly dependent on the local magnetic field strength. Much more detailed measurements of the plasma potential distribution will be reported in the near future.

VI. CONCLUSIONS

In summary, we have demonstrated that an emissive probe can be constructed and operated under pulsed conditions, and applied to transient plasmas like those created by HIPIMS. Alternating heating and plasma production has the advantage that the voltage drop along the heated filament is practically zero during the measurements, which greatly reduces the potential accuracy of the probe. Additionally, we do not need to worry about the magnetic field that is produced by the heating current, especially when the heated filament has a shape of a small coil, as in this study. The coil shape is convenient since filaments from commercial miniature light bulbs could be used, at a fraction of the cost of building or replacing custom probe filaments. The temperature and electron emission from the pulsed emissive probe was measured optically and electrically, respectively, indicating sufficient thermal inertia that the emission of electrons can be considered almost constant during the plasma pulse. Pulsed emissive probe operation was demonstrated by measuring the plasma potential distribution 30 mm from a niobium target under HIPIMS conditions. The results shown here indicate a potential drop of about -30 V in front of the racetrack region. This voltage drop is associated with the magnetic presheath, while most of the anode-cathode voltage drop is located in the thin (mm) sheath next to the target surface. Further measurements with this technique will reveal the complete potential distribution by positioning the emissive probe at positions of interest in the axial and radial directions.

ACKNOWLEDGMENTS

We gratefully acknowledge help by Dr. S. Lim and J. Wallig in assistance in probe construction and vacuum technology. A. Rauch thanks the Austrian Marshall Plan Foundation (www.marshallplan.at) for funding a scholarship. J. M. Sanders thanks the AFOSR for supporting his Ph.D. research. This work was done at Lawrence Berkeley National Laboratory with support by the U.S. Department of Energy under Contract No. DE-AC02-05CH11231.

Figure Captions

FIG. 1. A simplified schematic of the circuit used to pulse the probe's tungsten filament. A capacitor at the gate of the power MOSFET slows the turn-on time and reduces transients from switching the floating power supply.

FIG. 2 An image of the probe; the tungsten filament has a 30 diameter wire, a coil diameter of 240 μm, a coil length of about 1mm, and a total wire length of about 6 mm.

FIG. 3. The emissive probe tested in a HIPIMS experiment vacuum chamber. The probe's position is automatically controlled relative to the symmetry axis of the magnetron in 30 mm distance from the surface of the target. Plasma is generated by a planar magnetron that is driven by a HIPIMS pulse generator.

FIG. 4. A 20 ms pulse with a peak amplitude of 3.7 V is applied to the tungsten filament to heat it. The measurement was made differentially by placing two ground referenced probes at the positive and negative terminals of the probe. After about 10 ms, the i^2R loss in the filament has sufficiently heated it to cause electron emission. When heating is terminated, electron emission decays but at the decay rate that is sufficiently slow by comparison to a typical plasma pulse (600 μs in this case). The inset shows the decay during the plasma pulse.

FIG. 5. Normalized time-averaged intensity of blackbody radiation emitted from the hot emissive probe for different pulsed heating powers leading to different temperatures. The indicated temperature is calculated from fitting the intensity measurements (dense sequence of colored symbols) to fitting curves (black solid lines) of a black body radiator (note the emissivity is not important since we deal with normalized curves).

FIG. 6. As the duty cycle increases, the duration and amplitude of the heating pulse must be decreased and increased, respectively. Higher voltage drop at the filament would imply greater measurement uncertainty and plasma disturbance, emphasizing the benefit of the here-presented pulsed approach.

FIG. 7. Examples of current pulses for low and high power modes: the low power mode is shown here with -400 Volt applied to the Nb cathode for 800 μs at 0.33 Pa; the high power mode was observed by increasing the discharge voltage to -420 V at an argon pressure 0.28 Pa; in both cases, the repetition rate was set to 10 pulses per second. Note that the current scale for the low power mode was increased by a factor 30, compared to the high power mode, to better show the current shape. Time zero is define at the time when the voltage is applied to the target.

FIG. 8. The probe's bias was swept twice: once with heating pulses applied to the probe, once without. The measurements with the hot probe indicates a plasma potential of approximately -7.8V at a distance of 20 mm from the target.

FIG. 9. Probe current I_P as a function of time during the pulse for a given applied bias voltage V_B; the probe was positioned at r = 2 mm , z = 30 mm.

FIG. 10. *I-V* characteristic of the emissive probe, the probe was positioned at r = 2 mm from the target axis, and z = 30 mm from target surface. Bias sweeps are shown for two different phases of the discharge, the peak current and steady-state current, as indicated in Fig. 8.

FIG. 11. Plots of the plasma potential versus the radial distance r to the center of the magnetron. The probe position was 30 mm in front of the target. The measurement was performed over half the target (from 0 mm to 46 mm) and mirrored to facilitate understanding. The error bars indicate the standard deviation.

References

1. A. Y. Wong, G. Dimonte, J. R. Ferron, M. Y. Fukao, K. Jones, A. Kuthi, K. L. Lam, B. J. Leikind, R. W. Schumacher, H. Stephanian and R. G. Suchannek, Nucl. Instrum. Meth. Phys. Res. **207** (1-2), 207-221 (1983).
2. R. Schrittwieser and et al., Plasma Physics and Controlled Fusion **44** (5), 567 (2002).
3. N. Mahdizadeh and et al., Plasma Physics and Controlled Fusion **47** (4), 569 (2005).
4. I. Langmuir, Phys. Rev. **22** (4), 357 (1923).
5. Y. E. Wang, T. Intrator and N. Hershkowitz, Rev. Sci. Instrum. **56** (4), 519-524 (1985).
6. R. F. Kemp and J. M. Sellen Jr., Rev. Sci. Instrum. **37** (4), 455-461 (1966).
7. P. Balan, R. Schrittwieser, C. Ionita, J. A. Cabral, H. F. C. Figueiredo, H. Fernandes, C. Varandas, J. Adamek, M. Hron, J. Stockel, E. Martines, M. Tichy and G. Van Oost, Rev. Sci. Instrum. **74** (3), 1583-1587 (2003).
8. G. D. Hobbs and J. A. Wesson, Plasma Physics **9** (1), 85 (1967).
9. J. R. Smith, N. Hershkowitz and P. Coakley, Rev. Sci. Instrum. **50** (2), 210-218 (1979).
10. J. W. Bradley and et al., Plasma Sources Sci. Technol. **10** (3), 490 (2001).
11. A. Mishra, P. J. Kelly and J. W. Bradley, Plasma Sources Sci. Technol. **19** (4), 045014 (2010).
12. W. E. Yao, T. Intrator and N. Hershkowitz, Rev. Sci. Instrum. **56** (4), 519-524 (1985).
13. H. Shindo, M. Konishi and T. Tamaru, Rev. Sci. Instrum. **59** (9), 2002-2007 (1988).
14. U. Helmersson, M. Lattemann, J. Bohlmark, A. P. Ehiasarian and J. T. Gudmundsson, Thin Solid Films **513** (1-2), 1-24 (2006).
15. A. Anders, *Cathodic Arcs: From Fractal Spots to Energetic Condensation*. (Springer-Verlag, New York, 2008).
16. V. Kouznetsov, K. Macák, J. M. Schneider, U. Helmersson and I. Petrov, Surf. Coat. Technol. **122** (2-3), 290-293 (1999).
17. A. Anders, J. Andersson and A. Ehiasarian, J. Appl. Phys. **102** (11), 113303-113311 (2007).
18. A. Anders, Surf. Coat. Technol. **DOI: 10.1016/j.surfcoat.2011.03.081** (2011).
19. J. Vlček and K. Burcalová, Plasma Sources Sci. Technol. **19** (6), 065010 (2010).
20. G. Y. Yushkov and A. Anders, IEEE Trans. Plasma Sci **38** (11), 3028-3034 (2010).

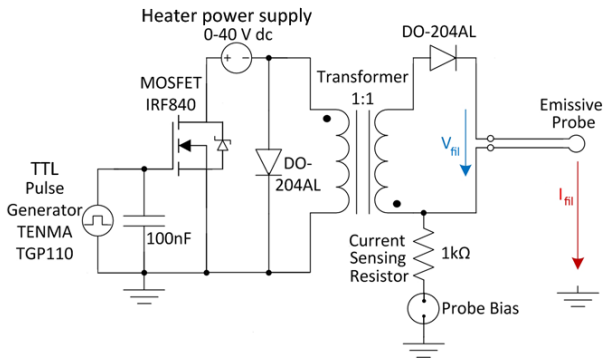
Heater power supply
0-40 V dc
DO-204AL
MOSFET
IRF840
Transformer
1:1
Emissive
Probe
V_{fil}
TTL
Pulse
Generator
TENMA
TGP110
DO-
204AL
I_{fil}
100nF
Current
Sensing
Resistor
1kΩ
Probe Bias

Fig. 1

Fig. 2

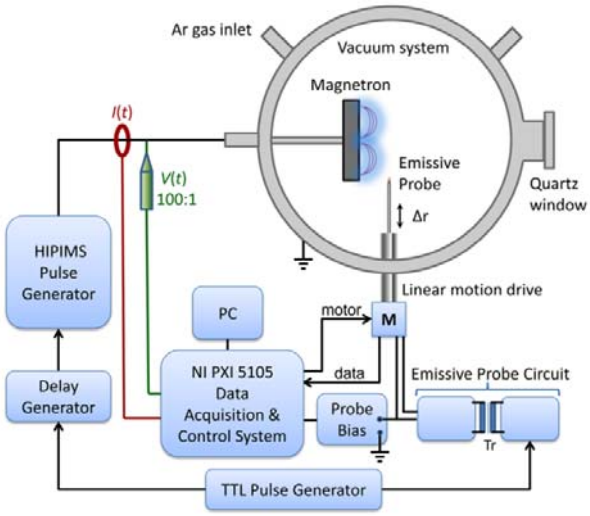
Ar gas inlet
Vacuum system
Magnetron
I(t)
V(t)
100:1
Emissive
Probe
Δr
Quartz
window
HIPIMS
Pulse
Generator
Linear motion drive
PC
motor
M
NI PXI 5105
Data
Acquisition &
Control System
data
Emissive Probe Circuit
Delay
Generator
Probe
Bias
Tr
TTL Pulse Generator

Fig. 3

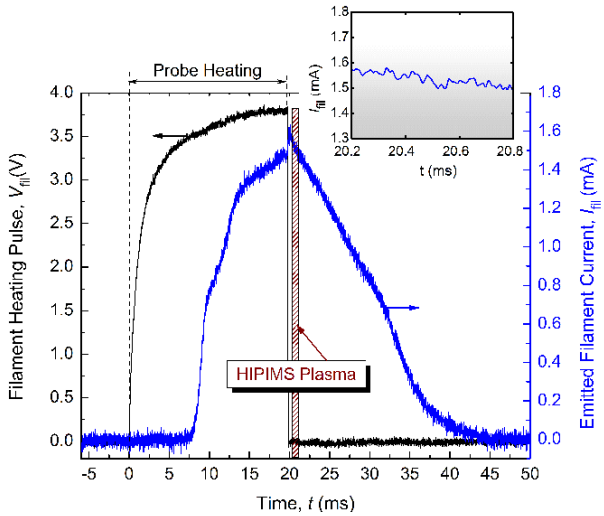
Probe Heating
HIPIMS Plasma
Filament Heating Pulse, V_{fil}(V)
Emitted Filament Current, I_{fil} (mA)
Time, t (ms)
I_{fil} (mA)
t (ms)

Fig. 4

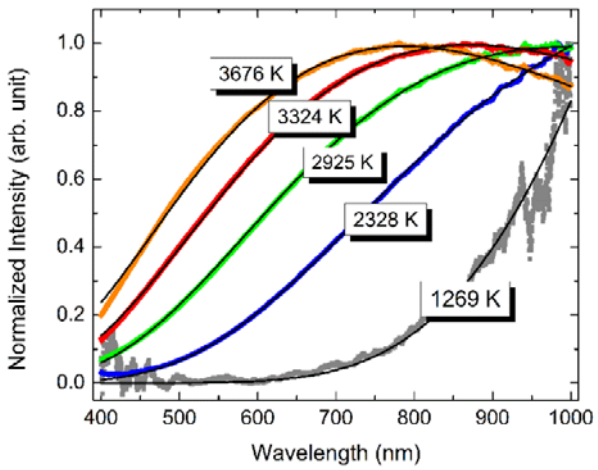
3676 K
3324 K
2925 K
2328 K
1269 K
Normalized Intensity (arb. unit)
Wavelength (nm)
0.0
0.2
0.4
0.6
0.8
1.0
400
500
600
700
800
900
1000

Fig. 5

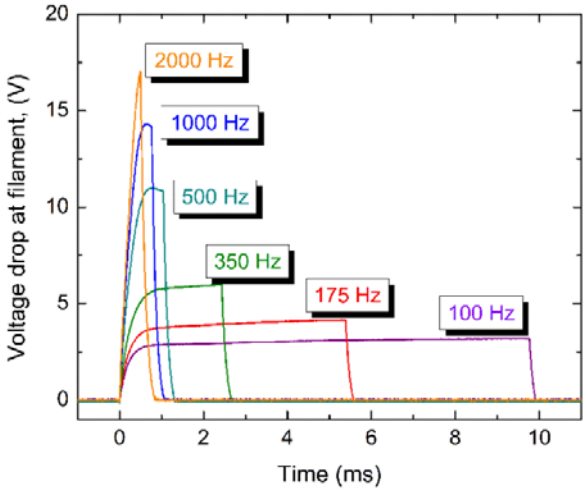
2000 Hz
1000 Hz
500 Hz
350 Hz
175 Hz
100 Hz
Voltage drop at filament, (V)
Time (ms)
0
5
10
15
20
0
2
4
6
8
10

Fig. 6

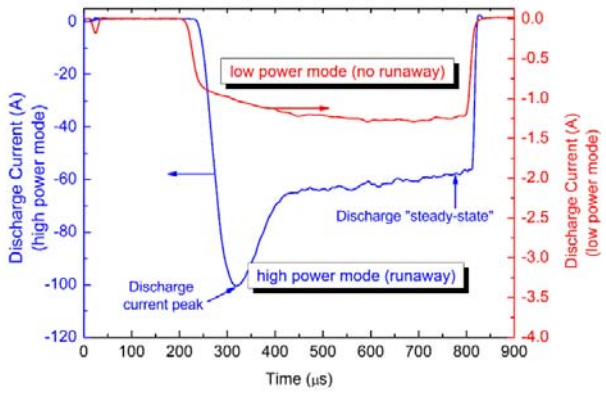
low power mode (no runaway)
high power mode (runaway)
Discharge "steady-state"
Discharge current peak
Discharge Current (A) (high power mode)
Discharge Current (A) (low power mode)
Time (μs)
0
-20
-40
-60
-80
-100
-120
0.0
-0.5
-1.0
-1.5
-2.0
-2.5
-3.0
-3.5
-4.0
0
100
200
300
400
500
600
700
800
900

Fig. 7

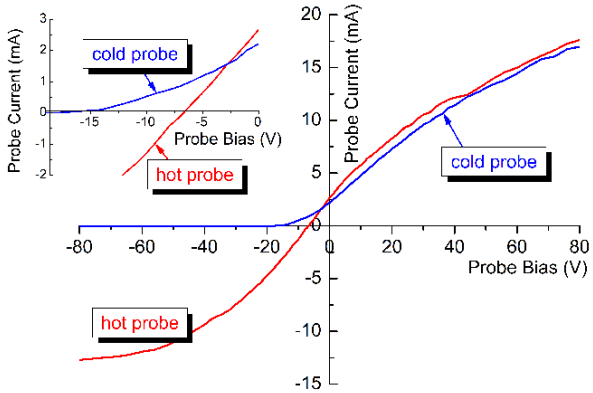
Probe Current (mA)
Probe Bias (V)
cold probe
hot probe
Probe Current (mA)
Probe Bias (V)
cold probe
hot probe

Fig. 8

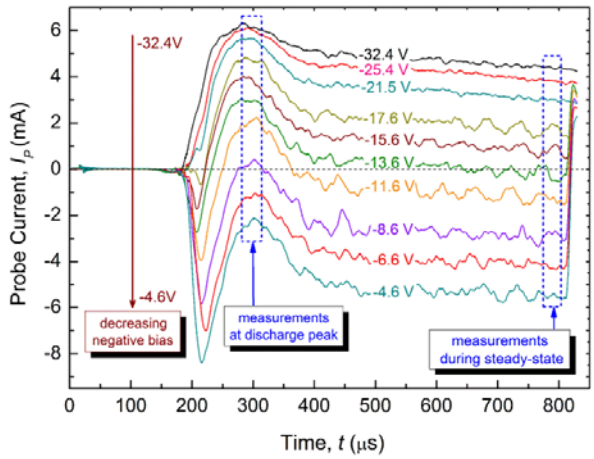
-32.4V
-4.6V
-32.4 V
-25.4 V
-21.5 V
-17.6 V
-15.6 V
-13.6 V
-11.6 V
-8.6 V
-6.6 V
-4.6 V
decreasing negative bias
measurements at discharge peak
measurements during steady-state
Probe Current, I_p (mA)
Time, t (μs)

Fig. 9

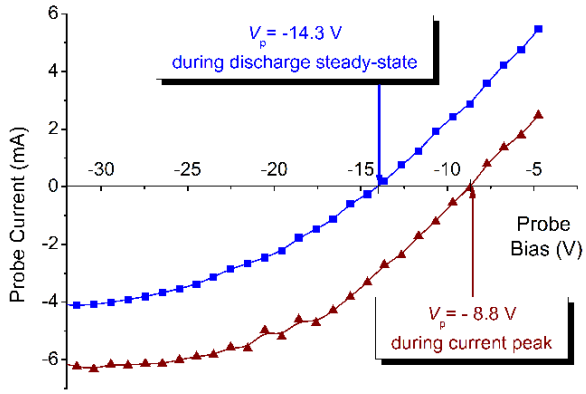
V_p = -14.3 V
during discharge steady-state
V_p = - 8.8 V
during current peak
Probe Current (mA)
Probe Bias (V)
6
4
2
0
-2
-4
-6
-30
-25
-20
-15
-10
-5

Fig. 10

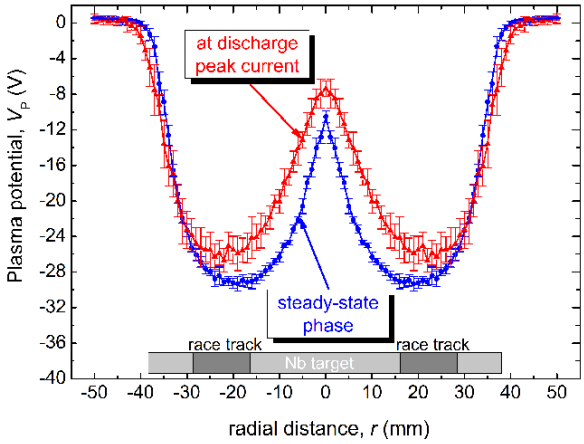
at discharge
peak current
steady-state
phase
race track
race track
Nb target
Plasma potential, V_p (V)
radial distance, r (mm)
0
-4
-8
-12
-16
-20
-24
-28
-32
-36
-40
-50
-40
-30
-20
-10
0
10
20
30
40
50

Fig. 11